V European Conference on Computational Fluid Dynamics
ECCOMAS CFD 2010
J. C. F. Pereira and A. Sequeira (Eds)
Lisbon, Portugal,14-17 June 2010

DIRECT NUMERICAL SIMULATION OF QUASI-STATIC MAGNETOHYDRODYNAMIC ANNULAR DUCT FLOW

S. Vantieghem* **and B. Knaepen***

* Statistical and Plasma Physics, Université Libre de Bruxelles, Campus Plaine, CP 231,
B-1050 Brussels, Belgium
e-mail: stvtiegh@ulb.ac.be

Key words: Magnetohydrodyanmics, Direct Numerical Simulation, Turbulence

Abstract. *We present results of numerical simulations of quasi-static magnetohydrodynamic duct flow in a toroidal duct of square cross-section. Such a study is motivated by a recent experimental investigation of the instability of the Hartmann layer [1]. This work forms a primary analysis of the velocity profile in such a device. In a first part, we consider the laminar flow, and present a comprehensive overview of both the main and secondary flow. Our study confirms and extends an earlier asymptotic analysis [7]. The second part treats the turbulent regime, and we focus mainly on the behavior of the shear layers. We show that the curvature creates an asymmetry in the level of turbulence between the convex and concave side layer. If a magnetic field is applied, only the concave shear layer remains unstable.*

1 Introduction

Magnetohydrodynamics (MHD) is the branch of physics which studies the coupling between the flow of electrically conducting fluids and electromagnetic fields. MHD flows are ubiquitous, as well in nature as in industrial applications. One can think for instance of the plasma in a solar corona, the liquid metal core of the Earth generating its dynamo, the flow of electrolytes in aluminum reduction cells, or the flow of liquid metal alloys in the heat exchangers of future fusion devices. Under some conditions, the induced magnetic field is negligible with respect to the externally imposed one. In this type of flows, the magnetic Reynolds number $R_m = \mu\sigma UL$ is small compared to one, where μ is the magnetic permeability and σ the electrical conductivity of the fluid, and U and L are typical length scales of the flow. The main signature of this regime, called *quasi-static MHD*, is that all variations along magnetic field lines tend to disappear.

In quasi-static MHD duct flows, different types of shear layers will emerge. On the one hand, we have the *Hartmann layer*, which appears at walls non-parallel to the magnetic field, and have a typical size of $M^{-1}L$, with M the *Hartmann number*, a nondimensional measure of the ratio between the Lorentz and the viscous force, which will be specified below. *Side layers* on the other hand, will arise in the vicinity of walls parallel to the field, and they have a typical thickness of the order of $M^{-1/2}L$.

The role of this different shear layers in the transition process is the subject of an ongoing debate within the quasi-static MHD community. Moresco et al. [1] performed friction factor measurements in a toroidal duct of square cross-section at high Hartmann number. Since the lion's share of the friction occurs in the Hartmann layer (at high M), a sudden change in the friction factor behavior was attributed to a change in the Hartmann layer. They found a transition in the friction factor behavior appears when the ratio between the Reynolds number Re and the Hartmann number is $Re/M \approx 380$. A numerical study of Krasnov et al [2], revealed that the transition in a straight channel occurs for the same critical value of Re/M. More recent numerical simulations [3] showed however that the nuclei of the instability in straight duct flow appear in the side layers.

The goal of this work is to contribute to a better understanding of the experiment of Moresco et al. The combination of Hartmann and Reynolds numbers used in the experiment, are however not accessible by direct numerical simulations at present. Therefore, we study here two other regimes, which are necessary for, or preliminary to further studies of the experiment. In a first part, we present the features of the laminar flow at moderate and high Hartmann number. In the second part, we compare the turbulent regime at modest Reynolds number between ordinary hydrodynamic and quasi-static MHD flows.

2 Governing equations

We consider the velocity field $\mathbf{u}$ of an incompressible flow in a toroidal duct of square cross-section with mean radius R and duct length $2L$. The axis of the torus is parallel to the y-direction (figure 1). The material parameters, like the density ρ, kinematic viscoisty

ν and the electrical conductivity σ are constant. The flow is subjected to an externally imposed, uniform magnetic field $\mathbf{B} = B_0 \mathbf{1}_y$. We will assume that the magnetic Reynolds

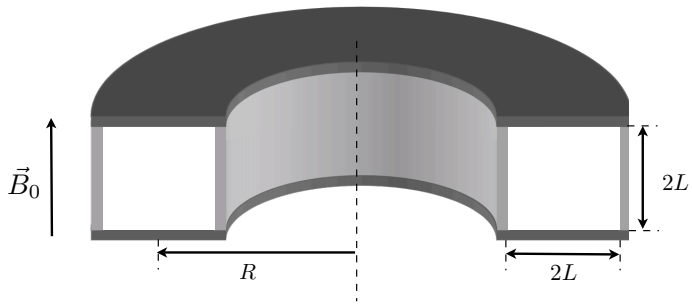

Figure 1: Sketch of the toroidal geometry. The color of the walls indicates their electrical conductivity: perfectly conducting (light grey), and perfectly insulating (dark grey).

number R_m is small compared to one, so that we can invoke the quasi-static approximation [4]. This means that the induced electric field can be derived from a scalar potential ϕ. Ohm's law takes then the following form:

$$\mathbf{j} = \sigma \left(-\nabla \phi + \mathbf{u} \times \mathbf{B} \right) \tag{1}$$

with $\mathbf{j}$ the induced current density. Charge relaxation times are typically very small, so that the constraint of charge conservation becomes $\nabla \cdot \mathbf{j} = 0$, which leads to:

$$\nabla^2 \phi = \nabla \cdot (\mathbf{u} \times \mathbf{B}) \tag{2}$$

The equation of mass and momentum conservation or the standard incompressible Navier-Stokes equations in which a Lorentz force term has been explicitly added:

$$\nabla \cdot \mathbf{u} = 0 \tag{3}$$

$$\rho \left(-\partial_t \mathbf{u} + \mathbf{u} \cdot \nabla \mathbf{u} \right) = -\nabla p + \rho \nu \nabla^2 \mathbf{u} + \mathbf{j} \times \mathbf{B} \tag{4}$$

We should still supply appropriate boundary conditions to close completely the problem (1)-(4). These are inspired by the aforementioned experiment [1]. All walls are no-slip walls; the Hartmann walls are perfect electrical insulators, and the side walls are perfectly conducting. Mathematically:

$$\mathbf{u} = 0, \partial_n \phi = 0 \qquad \text{at} \qquad y = \pm L \tag{5}$$

$$\mathbf{u} = 0, \phi = \pm V/2 \qquad \text{at} \qquad r = R \pm L \tag{6}$$

This means that the flow is driven by the Lorentz force caused by the potential difference between the side walls. An elementary calculation shows that the external potential difference generates a Lorentz force density, which is proportional to $\sigma V B_0 r^{-1}$.

The different cases that we will present, can be specified by merely three non-dimensional numbers: the well-known Reynolds number Re, the previously mentioned Hartmann number M and a geometrical parameter ξ, which is the ratio between the duct size and the mean radius of the torus:

$$Re = \frac{UL}{\nu} \tag{7}$$

$$M = B_0 L \sqrt{\frac{\sigma}{\rho\nu}} \tag{8}$$

$$\xi = \frac{L}{R} \tag{9}$$

These equations were solved using a finite-volume method, with a time-stepping method based on a canonical fractional-step algorithm [5].

3 Laminar flow

In this section, we will compare the velocity results for different values of the Hartmann number ($M = 25, 100, 400$) and the Reynolds number ($Re = 0, 100, 800$) for a fixed value of $\xi = 1/9$. Baylis et al. [6] derived that a sufficient condition for the flow to be laminar is $\xi^2 \times (Re^2/M^4) \ll 1$. In the present work, the maximum value of this product is about 0.08, and our simulations yielded steady results for all investigated parameter combinations. In figure 2, we display the streamwise velocity profile along the duct's centerline in radial direction, rescaled with the following reference velocity U_0:

$$U_0 = \frac{V}{B_0 R \log\left(\frac{R+L}{R-L}\right)} \tag{10}$$

It shows that the centrifugal force has only a significant influence at the lowest value of M. Furthermore, we see that the velocity profile decreases with increasing radial coordinate in the core region. This is a reflection of the $1/r$-behavior of the external forcing mechanism. At the highest Hartmann number, we see that small overspeed zones appear at the border between the side layers and the core.

In figure 3, we show the magnitude and streamlines of the secondary flow field. The magnitude U_s has been rescaled with the reference velocity U_0, i.e.: $U_s = U_0^{-1}\sqrt{v^2 + u_r^2}$, with v and u_r respectively the y-component and the radial component of the velocity field $\mathbf{u}$. The streamlines are isolines of a stream function ψ, which is the solution of a Poisson equation with Dirichlet conditions $\psi = 0$ on all the walls:

$$\nabla^2 \psi = \omega_\theta \tag{11}$$

with ω_θ the streamwise component of the vorticity. The magnitude of U_s shows us that the ratio between the magnitudes of the secondary and main flow scales as M^{-2}. Furthermore,

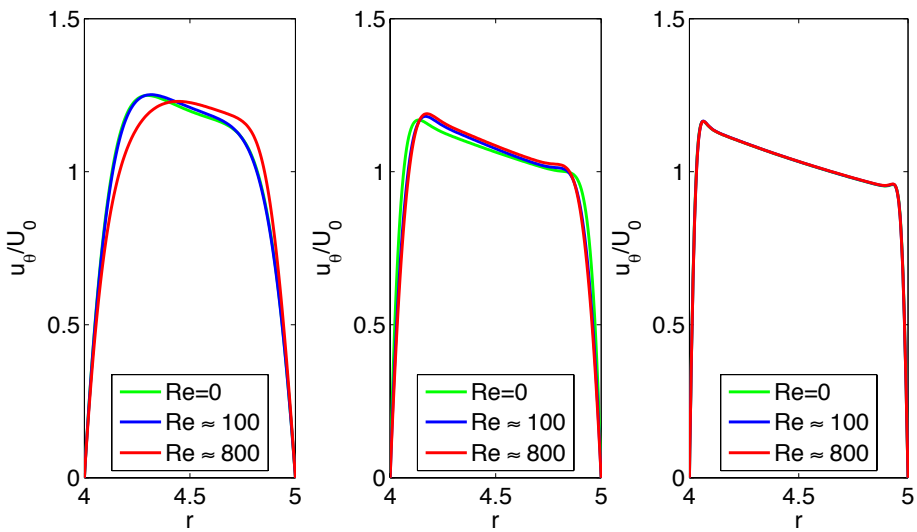

Figure 2: Streamwise velocity profile along the radial centerline of the duct for different values of M and Re. $M = 25$ (left), $M = 100$ (center), $M = 400$ (right).

we see that this secondary flow is the strongest in the Hartmann layers. These results are in good agreement with an earlier asymptotic analysis of Tabeling et al. [7]. At $M = 25$, we see that the secondary flow takes the form of two counter-rotating Ekman vortices (only one is displayed for reasons of symmetry). At higher values of M, the structure becomes more complex, with two subvortices emerging within the main Ekman vortex cell. For $M = 400$ at last, we see that small side layer vortices appear at the outer and inner walls, which were also predicted by [7]; these are however very weak and not discernible in the profile of U_s. Therefore, we show a detail of U_s near the inner and outer walls in figure 4, in which the radial coordinate r has been rescaled into units of side layer thickness: $s_\pm = \sqrt{M}(R \pm L \mp r)$. The inner vortex is significantly stronger than the outer one.

4 Turbulent flow

In this section, we want to compare the nature of the turbulent behavior between ordinary hydrodynamic and magnetohydrodynamic flows. We will consider two values of the Hartmann number: $M = 0$,$M = 30$. In both flows the Reynolds number is of the order $Re \approx 3900 - 4000$. In the hydrodynamic case, a steady pressure gradient with a $1/r$-behavior was imposed to drive the flow. The value of the parameter ξ was $1/18$.

In figure 5, we compare the average of the mean streamwise velocity, $\overline{u_\theta}$, and of its fluctuating part, $\overline{u_\theta}^{rms}$, between both Hartmann numbers. The mean velocity profiles reveal that the centrifugal forces shift the velocity maximum outwards (with respect to the laminar results), and that the magnetic field tends to suppress all variations along its field lines. Without magnetic field, higher velocities also occur near the top and bottom

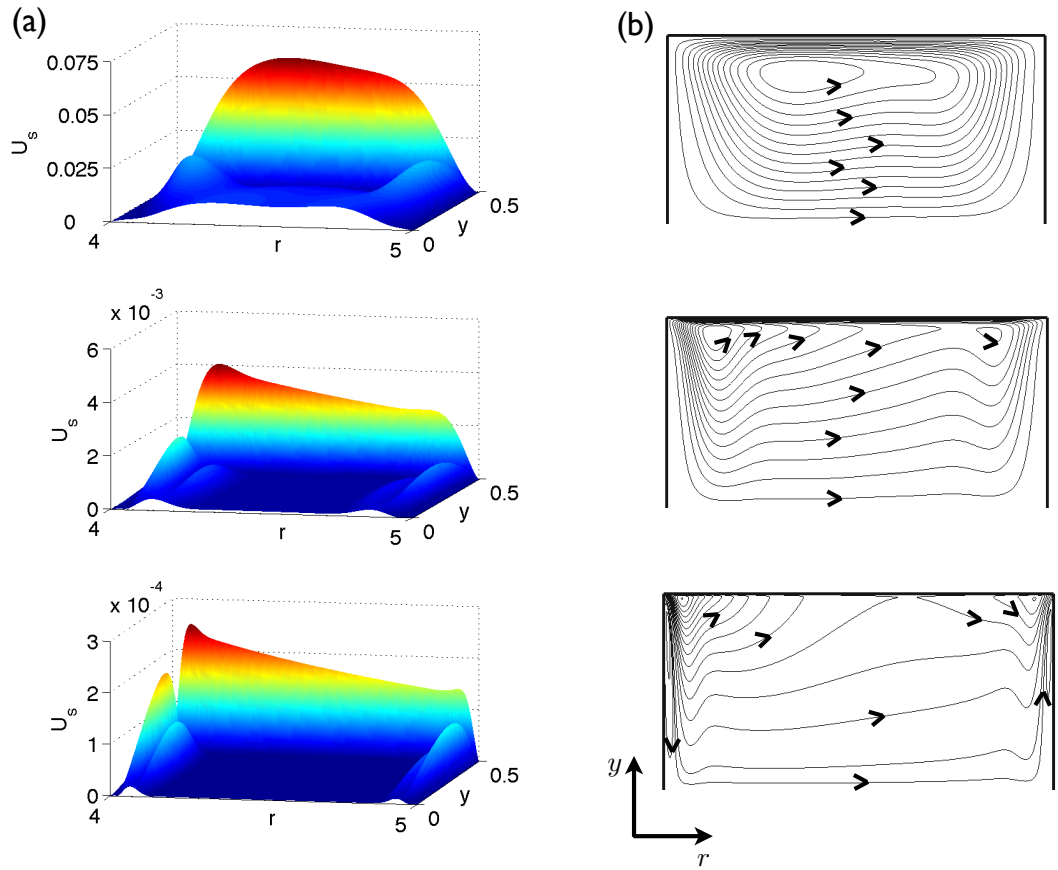

Figure 3: Magnitude (a) and streamlines (b) of the secondary flow field. $M = 25$ (top), $M = 100$ (center), $M = 400$ (bottom).

walls. The magnitude of $\overline{u_\theta}^{rms}$ can be interpreted as a measure for the local turbulence intensity. In the hydrodynamic case, we see that all boundary layers are unstable, but with a significant asymmetry between the concave and convex side of the duct. This feature was already noticed in earlier studies of turbulent curved channel flow [8]. When a magnetic field is applied, we see that the turbulence disappears everywhere, except in the concave side layer. This supports the findings of [xx], who found that the instability of the Hartmann layers is precursed by an instability of the side layers.

5 Conclusions

In this work, we presented a primary analysis of the quasi-static MHD flow in a toroidal duct with square cross-section by means of numerical simulations. In the laminar case, the magnetic field suppresses the effect of the centrifugal force, and has a dramatic effect on the structure of the secondary flow. The most striking feature is that side layer vortices emerge at sufficiently high Hartmann number. The simulations of the turbulent

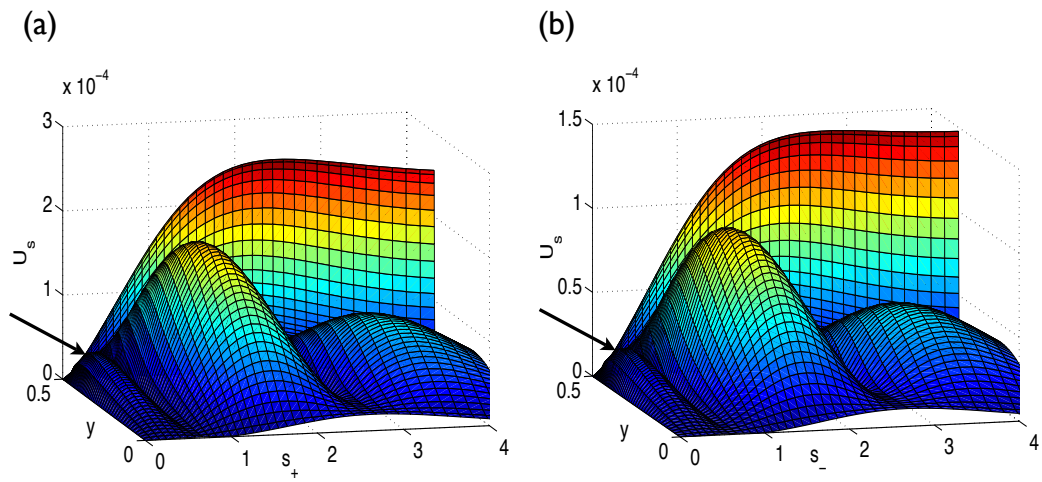

Figure 4: Magnitude of the secondary flow field U_s near the inner and outer corner of the duct for $M = 400$. Arrows indicate the location of the side layer vortices.

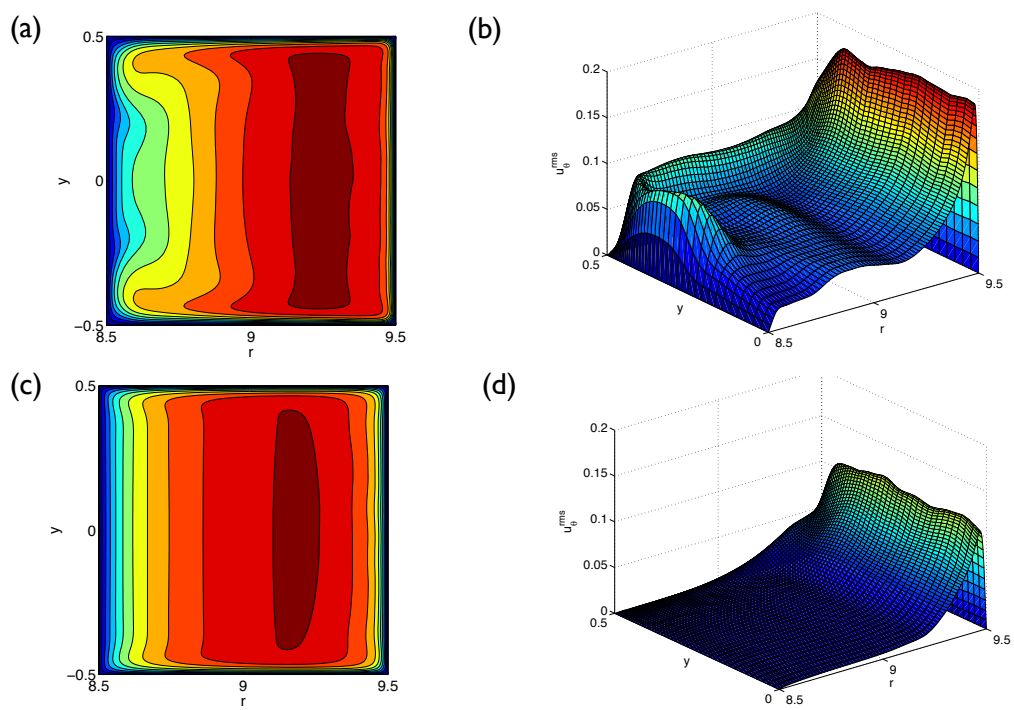

Figure 5: Statistics of the turbulent flow: mean streamwise velocity $\overline{u_\theta}$ (a,c) and mean fluctuating velocity $\overline{u_\theta}^{rms}$ (b,d) for the cases $M = 0$ (a,b) and $M = 30$ (c,d).

cases illustrated the aligning effect of the magnetic field, and the asymmetric nature of the turbulence between the convex and concave side layers. When a magnetic field was applied, we saw that the overall level of turbulence was suppressed, and only the concave side layer remained unstable.

REFERENCES

[1] P. Moresco and T. Alboussière, Experimental study of the instability of the Hartmann layer, *J. Fluid Mech.*, **504**, 167-181 (2004).

[2] D. S. Krasnov, E. Zienicke, O. Zikanov, T. Boeck and A. Thess, Numerical study of the instability of the Hartmann layer, *J. Fluid Mech.*, **504**, 183-211 (2004).

[3] D. S. Krasnov and T. Boeck, *private communication*.

[4] P. H. Roberts, An introduction to magnetohydrodynamics, *American Elsevier Publishing Company Inc* (1967).

[5] J. Kim and P. Moin, Application of a fractional-step method to the incompressible Navier-Stokes equations, *J. Comp. Phys.*, **59**, 308-323 (1985).

[6] J. A. Baylis and J. C. R. Hunt, MHD flow in an annular channel; theory and experiment, *J. Fluid Mech.*, **48**, 423-428 (1971).

[7] P. Tabeling and J.P. Chabrerie, Magnetohydrodynamic secondary flows at high Hartmann number, *J. Fluid Mech.*, **103**, 225-239 (1981).

[8] M. Nagata and N. Kasagi, spatio-temporal evolution of coherent vortices in wall turbulence with streamwise curvature, *J. Turbulence.*, **1**, 17-17 (2004).